

# UC Berkeley

## Working Papers

### Title

Discretization and Validation of the Continuum Approximation Scheme for Terminal System Design

### Permalink

<https://escholarship.org/uc/item/9dm7v0cn>

### Authors

Ouyang, Yanfeng  
Daganzo, Carlos F.

### Publication Date

2003-10-01

Institute of Transportation Studies  
University of California at Berkeley

**Discretization and Validation of the Continuum Approximation Scheme for Terminal System Design**

**Yanfeng Ouyang and Carlos F. Daganzo**

WORKING PAPER  
UCB-ITS-WP-2003-2

October 2003  
ISSN 0192 4141

**DISCRETIZATION AND VALIDATION OF THE CONTINUUM  
APPROXIMATION SCHEME FOR TERMINAL SYSTEM DESIGN**

Yanfeng Ouyang and Carlos F. Daganzo

Institute of Transportation Studies

Department of Civil and Environmental Engineering

University of California at Berkeley, CA 94720

Working Paper

August 1st, 2003

# **DISCRETIZATION AND VALIDATION OF THE CONTINUUM APPROXIMATION SCHEME FOR TERMINAL SYSTEM DESIGN**

Yanfeng Ouyang and Carlos F. Daganzo

Institute of Transportation Studies and Department of Civil and Environmental Engineering

University of California at Berkeley, CA 94720

(August 1st, 2003)

## **ABSTRACT**

This paper proposes an algorithm that automatically translates the "continuum approximation" (CA) recipes for location problems into discrete designs. It is applied to terminal systems but can also be used for other logistics problems. The study also systematically compares the logistics costs predicted by the CA approach with the actual costs for discrete designs obtained with the automated procedure. Results show that the algorithm systematically finds a practical set of discrete terminal locations with a cost very close to that predicted. The paper also gives conditions under which the CA cost formulae are a tight lower bound for the exact minimal costs.

1. BACKGROUND .....	1
2. THE MODEL AND ALGORITHM.....	4
2.1. A Disk Model.....	5
2.2. The Algorithm.....	6
3. ILLUSTRATIONS .....	8
3.1. Convergence Test.....	8
3.2. Practical Examples.....	8
4. A LOWER BOUND .....	12
5. CONCLUSION.....	16
ACKNOWLEDGEMENTS .....	17
REFERENCES .....	18
LIST OF FIGURES .....	20



# DISCRETIZATION AND VALIDATION OF THE CONTINUUM APPROXIMATION SCHEME FOR TERMINAL SYSTEM DESIGN

Yanfeng Ouyang and Carlos F. Daganzo

Institute of Transportation Studies and Department of Civil and Environmental Engineering

University of California at Berkeley, CA 94720

(August 1st, 2003)

## 1. BACKGROUND

Designing a physical distribution system for minimal logistics cost is a complex task. The objective function usually includes complicated cost expressions for the various distribution stages, i.e., *inbound costs* for deliveries into the terminals, *outbound costs* for deliveries from terminals to customers, and *terminal costs* for handling within terminals. Furthermore, the decision variables are usually discrete and very numerous, including the number of terminals, their locations, delivery routes, schedules, and the allocation of customers to terminals.

The paper focuses on the strategic design of a terminal system in a continuous service area  $S$ , where customer demand is distributed with a spatial density  $\lambda(x)$ ,  $x \in S$ . The goal is to find a set of terminal locations,  $\mathbf{x} = \{x_1, x_2, \dots, x_N\}$ , and a partition of  $S$  into a set of *influence areas* served by these terminals,  $\mathbf{I} = \{I_1, I_2, \dots, I_N\}$ , that minimize the total logistics cost,  $Z_D(\mathbf{x}, \mathbf{I})$ . The number of terminals  $N$  is itself a decision variable. The minimization problem is:

$$\begin{aligned} \text{Min } Z_D(\mathbf{x}, \mathbf{I}) &= \sum_{i=1}^N \left( \int_{I_i} z_D(x, x_i, I_i) \cdot \lambda(x) dx \right), & (1) \\ \text{s.t. } x_i &\in S, \quad i = 1, 2, \dots, N, \\ I_i \cap I_j &= \emptyset \text{ for } \forall i \neq j, \\ \bigcup_i I_i &= S, \end{aligned}$$

where  $z_D(x, x_i, I_i)$  is the cost of serving a unit of demand at  $x \in I_i$  via a terminal at  $x_i$ .

A simpler version of (1) is called in the applied mathematics literature the “optimal resource allocation problem” (Okabe et al., 1992, Du et al., 1999.) These problems also allow point-like service facilities to be located among a continuum of customers. However, for the problems to be tractable,  $z_D$  must be a simple function of a norm,  $\|x-x_i\|$ ; e.g.  $\|x-x_i\|^2$ . Unfortunately, these simple forms are not realistic for typical logistics problems (e.g., including inbound costs).

Facility location problems can also be formulated by considering a finite number of possible locations for customers and terminals. Optimal locations are then selected with a mixed-integer program. An extensive literature also exists on this subject; see e.g., Daskin (1995) and Drezner and Hamacher (2002). This approach is effective if the number of candidates is small, but for a problem like (1), the number of possible choices is so large that a discrete optimization process is not practical even if done heuristically.

To circumvent some of those drawbacks and building on the work in Newell (1971 and 1973), Daganzo and Newell (1986) proposed a continuum approximation (CA) approach for terminal system design. It was argued in this reference that a near optimum solution should have influence areas as “round” as possible, with terminals located near

their centers. It was also argued that if in addition  $\lambda(x)$  varies slowly with  $x$ , and the areas  $|I_i|$  can be approximated by a slow-varying function of  $x$ ,  $A(x)$ , such that  $|I_i| \cong A(x)$  if  $x \in I_i$ , then the set function  $z_D(x, x_i, I_i)$  in (1) can be approximated by a simpler function of two real arguments,  $z_C(x, A(x))$ .

The function  $A$  is a decision variable representing the desired influence area size for locations near  $x$ . With this approximation, (1) can be replaced by

$$\text{Min } Z_C(A) = \int_S z_C(x, A(x)) \cdot \lambda(x) dx, \quad (2)$$

where  $Z_C(A)$  is a functional of  $A$ . More details about the procedure for obtaining  $z_C$  from  $z_D$  are given in Sec. 3, and also in Daganzo (1999).

The advantage of (2) is that it can be optimized point by point, by finding the value of  $A(x)$  that minimizes  $z_C(x, A(x))$  at every  $x$ . This result is denoted  $A^*(x)$ , and the corresponding cost  $Z_C^*(A^*)$ . One then looks for a partition of  $S$  with “round” influence areas such that:

$$|I_i| \cong A^*(x), \quad \forall x \in I_i, \quad (3)$$

and for a set of centrally located terminals. The hope is that the discrete solution so identified,  $\{\mathbf{x}_C, \mathbf{I}_C\}$ , will satisfy  $Z_D(\mathbf{x}_C, \mathbf{I}_C) \cong Z_C^*(A^*)$ . The extent to which this happens is explored in this paper. The paper also proposes a discretization algorithm to obtain the

solution  $\{\mathbf{x}_C, \mathbf{I}_C\}$ , since to the authors' best knowledge, no systematic procedure has yet been proposed for the discretization step.

The closest literature deals with surface-fitting problems, and is described under the rubric "location optimization of observation points for estimating the total quantity of a continuous spatial variable" in Okabe et al. (1992). Unfortunately, the solutions to these kinds of problems (e.g., as in Hori, H. and Nagata, M., 1985) turn out to be *Voronoi tessellations*, where the partitioned sub-areas may not be round with proper sizes. Thus, this literature is not suitable for our purposes.

Numerical examples show that the feasible designs obtained with the proposed algorithm indeed exhibit costs  $Z_D(\mathbf{x}_C, \mathbf{I}_C)$  very close to the CA prediction  $Z_C^*(A^*)$ . The paper also gives sufficient conditions under which  $Z_C^*(A^*)$  is a tight lower bound for the exact optimal system costs. Since  $Z_D(\mathbf{x}_C, \mathbf{I}_C)$  and  $Z_C^*(A^*)$  are close to each other, the optimality gap between  $Z_D(\mathbf{x}_C, \mathbf{I}_C)$  and the true optimum should be small under these conditions.

This paper is organized as follows. Section 2 develops the discretization algorithm; section 3 shows the numerical examples; and section 4 shows the conditions under which  $Z_C^*(A^*)$  bounds from below the true minimum. A final section discusses generalizations.

## 2. THE MODEL AND ALGORITHM

As discussed before, a near optimum design  $\{\mathbf{x}_C, \mathbf{I}_C\}$  should: (i) satisfy the size requirement (3), (ii) have influence areas as round as possible, and (iii) have terminals

located near the centers of the influence areas. (We assume from now on that distances are given by the Euclidean metric.)

### 2.1. A Disk Model

To capture (ii) and (iii), we will imagine that each influence area contains a round disk centered at the terminal, and instead of  $\{\mathbf{x}_C, \mathbf{I}_C\}$  we will look for a set of  $N$  non-overlapping disks, where  $N \cong \int_S [A^*(x)]^{-1} dx$ . By sliding the disks within  $S$ , different designs can be obtained. Two examples are displayed in Figure 1. We use  $\mathbf{r}(\mathbf{x}) = \{r(x_i)\}$  for the set of disk radii; see dotted arrows. For a good design, disks should jointly cover most of  $S$  without protruding outside it, as shown in Figure 2(a). Since each influence area must contain one disk, this ensures that the influence areas are “round”. In addition, for a good design, the area of each disk should be as close as possible to  $A(x^*)$ ; i.e.,

$$r(x_i) \approx \sqrt{\frac{A^*(x_i)}{\pi}}, \quad i=1,2,\dots,N. \quad (4a)$$

It should be possible to satisfy these two conditions simultaneously since there always are many ways to cover most of  $S$  with disks of different sizes, as illustrated by Figure 2(b).

Of course, since disks cannot tessellate convex Euclidean regions, we cannot expect the equality in (4a) to be satisfied exactly. Therefore, we look instead for radii that satisfy

$$r(x_i) = \sqrt{\frac{A^*(x_i)}{k}}, \quad i=1,2,\dots,N, \quad (4b)$$

for  $k$  as small as possible. (Given our definition for  $N$ ,  $k \geq \pi$ .)

To automate the sliding procedure, we now introduce two types of repulsive “forces” that act on the centers of the disks. The first type, terminal force  $F_T$ , acts along the line connecting the centers of overlapping disks. The other type, boundary force  $F_B$ , acts on disks touching the boundary, pointing toward the interior of  $S$  in a direction normal to the boundary. Solid arrows in Figure 1(a) depict these forces.

Figure 3 defines our choices for the magnitudes of  $F_T$  and  $F_B$ . They depend on  $\mathbf{r}(\mathbf{x})$ , vanishing when no disks overlap or touch the boundary. We use  $(N+1)f$  for the magnitude of  $F_B$ , where  $f$  is the maximal value of  $F_T$ , to ensure that disks are never pushed out of  $S$ . We call a pattern with zero forces an *equilibrium*. The disk centers of an equilibrium give  $\mathbf{x}_C$ . This is sufficient to obtain a solution since  $S$  can then be easily partitioned into influence areas,  $\mathbf{I}_C$ , that contain the disks as will be explained shortly. Although such equilibrium solution  $\{\mathbf{x}_C, \mathbf{I}_C\}$  may not be unique, it should satisfy the near-optimality requirements (i) – (iii).

## 2.2. The Algorithm

The forces defined above are used to slide the disks within  $S$  for small distances, while  $\mathbf{r}(\mathbf{x})$  and the forces themselves are updated. The algorithm stops when all forces vanish. An equilibrium obviously exists and can be found for a sufficiently large  $k$ . Conversely, an equilibrium will not exist if  $k$  is too small. Therefore, the algorithm increases  $k$  by a small increment,  $\Delta k$ , if the current value does not yield an equilibrium.

Step sizes for disk movements should not be too large for fast convergence. One could use constant step sizes comparable with the tolerance level  $\varepsilon$  (in distance units) or, even better, gradually decreasing step sizes; e.g.,  $\mu/m$ , where  $\mu$  is an initial step size and  $m$  is the iteration count.

Even for reasonably large  $k$ , this algorithm may not converge to an equilibrium if we encounter sets of *degenerate* terminal locations (also called singular points in Okabe et al., 1992). This happens for example if points are on a straight line that intersects the boundaries of  $S$  orthogonally. In this case points would remain trapped on this line, since all ensuing terminal movements would have to be along the line. Fortunately, such degeneracy is usually unstable, and can be eliminated by small location perturbations. Therefore we add perturbations of random direction with a displacement size  $\delta < \varepsilon$  at each step of the procedure.

Once an equilibrium has been obtained,  $S$  is partitioned into  $\mathbf{I}_C$  with a *weighted-Voronoi tessellation* (WVT) that ensures each  $I_i$  contains one entire disk. The recipe is simple: first partition  $S$  into very small squares, and then allocate each square to one  $I_i$

with the rule  $i = \arg \min_j \left\{ \frac{\|x - x_j\|}{r(x_j)} \right\}$ , where  $x$  is the center of the square. This rule ensures

that every disk is a subset of its influence area.

In summary, the steps of the algorithm are:

- 1) Choose  $N$  arbitrary locations in area  $S$  and initialize all parameters: tolerance  $\varepsilon$ , initial step size  $\mu$ , perturbation size  $\delta$ , and increment for  $k$ ,  $\Delta k$ ; set initial  $k \cong \pi$  and  $m=1$ ;

- 2) Calculate the disk sizes with (4b) and then the forces on every terminal as per Figure 3; if all the forces equal zero (equilibrium reached), go to step 5); otherwise, move each terminal along the direction of its resultant force by a step size  $\mu/m$ , and add a random-direction perturbation of size  $\delta$ .
- 3) If  $\mu/m < \varepsilon$ , reset  $m = 0$ , and increase  $k$  by  $\Delta k$  ;
- 4)  $m = m+1$ ; go to step 2);
- 5) Tessellate  $S$  with the WVT recipe. ■

### 3. ILLUSTRATIONS

#### 3.1. Convergence Test

The algorithm's convergence is illustrated with a problem that has a known solution, using the poly-hexagonal region  $S$  of Figure 4(a). The side of each hexagon in  $S$  equals  $1/\sqrt{3}$ . If  $A^*(x) = \sqrt{3}/2$  and  $N = 7$ , then the partition in Figure 4(a) is optimal.

The initial locations are arbitrarily generated and shown in Figure 4(b). For simplicity a constant step size  $\mu = 0.01$  is used. Figure 4(c) shows an intermediate result, and Figure 4(d) finds the equilibrium, which was achieved after 440 iterations. Note that the weighted-Voronoi tessellation corresponding to Figure 4(d) matches in Figure 4(a). Thus, the algorithm performs as expected.

#### 3.2. Practical Examples

In this section we use practical examples to further illustrate how the algorithm translates  $A^*(x)$  into discrete designs  $\{\mathbf{x}_C, \mathbf{I}_C\}$ . The exact costs of the design,  $Z_D(\mathbf{x}_C, \mathbf{I}_C)$ , are then compared to the estimated costs  $Z_C^*(A^*)$ .

Daganzo (1999, Section 5.3.5) gives an example of terminal system design, in which customers are uniformly distributed in an  $L \times L$  square area  $S$ . They are served with one transshipment from a depot at one corner of  $S$ . Line-haul vehicles with infinite capacity shuttle between the depot and the terminals. Local delivery vehicles have a small capacity  $v_{\max}$ , travel full, and visit only one customer per delivery.

If we only consider inventory and transportation costs (both inbound and outbound), and ignore fixed costs such as terminal facility rents, the formula for  $z_D(x, x_i, I_i)$  in (1) is (Daganzo, 1999):

$$z_D(x, x_i, I_i) = 2 \left( \frac{a'b'R(x_i)}{\int_{I_i} \lambda(x) dx} \right)^{\frac{1}{2}} + \frac{av_{\max}}{\lambda(x)} + \frac{1.5\sqrt{\pi}b}{v_{\max}} s(x, x_i). \quad (5)$$

┌-----┐ ┌-----┐  
Inbound Outbound  
costs costs

In (5),  $a'$ ,  $b'$ ,  $a$ ,  $b$  are cost parameters,  $R(x)$  is the distance from point  $x$  to the depot, and  $s(x, x_i)$  is the outbound delivery distance from  $x_i$  to  $x$ .

On the other hand, the expression for  $z_C(x, A(x))$  in (2), as shown in (Daganzo, 1999), is:

$$z_C(x, A(x)) = 2 \left( \frac{a'b'R(x)}{\lambda(x)A(x)} \right)^{\frac{1}{2}} + \frac{av_{\max}}{\lambda(x)} + \frac{b}{v_{\max}} A^{\frac{1}{2}}(x). \quad (6)$$

Formula (6) is derived from (5) by approximating the terminal throughput  $\int_{I_i} \lambda(x) dx$  appearing in the first term with  $\lambda(x)A(x)$ , and  $s(x, x_i)$  with the average a delivery

distance  $\frac{2}{3\sqrt{\pi}}\sqrt{A(x)}$  in a hypothetical circular influence area of size  $A(x) \approx |I_i|$ . The idea is to express every item in (5) as a local property of point  $x$ . This *local approximation* device can be used with more general forms of (5). Experience shows that it works well when  $\lambda(x)$  and  $I_i$  vary slowly with position, as mentioned in Section 1. Two scenarios with different demand density functions  $\lambda(x)$  are now used to demonstrate this idea. The results are then formalized in Section 4.

**Scenario 1:** Consider homogeneous demand  $\lambda(x) = 1, \forall x \in S$ , and also assume that  $v_{\max} = b = b' = a' = b' = 1$ . Then  $A^*(x)$  is obtained by minimizing (6), and the result is:

$$A^*(x) = \left( \frac{2v_{\max}}{b} \right) \left( \frac{a'b'R(x)}{\lambda} \right)^{\frac{1}{2}} = 2R^{\frac{1}{2}}(x). \quad (7)$$

Substituting (7) into (6) and (6) into (2), we then find:

$$Z_C^*(A^*) = \int_S \lambda(x) \cdot z_C(x, A^*(x)) dx = \int_S \left( 1 + 2\sqrt{2} \cdot R^{\frac{1}{4}}(x) \right) dx. \quad (8)$$

If we now combine (1) and (5), the result is:

$$Z_D(\mathbf{x}, \mathbf{I}) = \sum_{i=1}^N \left( 2R^{\frac{1}{2}}(x_i) \cdot |I_i|^{\frac{1}{2}} + |I_i| \right) + 1.5\sqrt{\pi} \cdot \sum_{i=1}^N \left( \int_{I_i} s(x, x_i) dx \right), \quad (9)$$

Our algorithm uses (7) as an input. The set of discrete designs  $\{\mathbf{x}_C, \mathbf{I}_C\}$  obtained with it, and the associated values of  $Z_C^*(A^*)$ , and  $Z_D(\mathbf{x}_C, \mathbf{I}_C)$  given by (8) and (9) for various  $L$  are shown in Figure 5(a)–(d).

The difference between  $Z_C^*(A^*)$ , and  $Z_D(\mathbf{x}_C, \mathbf{I}_C)$  is quite small: 2.4% for  $L=5$ , 0.8% for  $L=7$ , 0.9% for  $L=10$ , and 0.9% for  $L=25$ . These relative differences would be even smaller if other fixed costs were also included in our cost expressions.

**Scenario 2:** Assume now an inhomogeneous demand such that  $\lambda(x) = R^{-\frac{1}{2}}(x)$ ,  $\forall x \in S$ .

All other parameters remain the same. Now we have

$$A^*(x) = 2R^{\frac{3}{4}}(x), \quad (10)$$

$$Z_C^*(A^*) = \int_S \lambda(x) \cdot z_C(x, A^*(x)) dx = \int_S \left(1 + 2\sqrt{2}R^{-\frac{1}{8}}(x)\right) dx, \quad (11)$$

and

$$Z_D(\mathbf{x}, \mathbf{I}) = 2 \sum_{i=1}^N \left( R^{\frac{1}{2}}(x_i) \cdot \sqrt{\int_{I_i} \lambda(x) dx} \right) + \sum_{i=1}^N \left( |I_i| + 1.5\sqrt{\pi} \int_{I_i} \lambda(x) s(x, x_i) dx \right). \quad (12)$$

The set of designs and associated costs are now shown in Figure 6(a)-(d).

The cost differences are 2.6%, 2.3%, 1.6%, and 0.7% respectively. They are approximately the same as those in scenario 1. This shows that the cost differences are insensitive to gradual demand variations.

In all the examples the algorithm produced the solution in less than 30 minutes on a 1.7 GHz PC with our choice of parameters. Note too that in both examples,  $Z_C^*(A^*)$  is slightly smaller than  $Z_D(\mathbf{x}_C, \mathbf{I}_C)$ . This is not necessarily true in general (Daganzo, 1999), but is quite common. Section 4 below gives sufficient conditions under which  $Z_C^*(A^*)$  is a lower bound for the costs of a design  $\{\mathbf{x}, \mathbf{I}\}$ .

#### 4. A LOWER BOUND

We consider in this section a generalization of (5) of the following form:

$$z_D(x, x_i, I_i) = z^i \left( R(x_i), \int_{I_i} \lambda(x) dx \right) + z^o(s(x, x_i), \lambda(x)), \quad (12)$$

where  $z^i$  and  $z^o$  are ordinary functions of two arguments. For this case, the local approximation device yields:

$$z_C(x, A(x)) = z^i(R(x), \lambda(x)A(x)) + z^o\left(\frac{2}{3\sqrt{\pi}}\sqrt{A(x)}, \lambda(x)\right). \quad (13)$$

We can now prove the following theorem.

**Theorem:**  $Z_C(A^*) \leq Z_D(\mathbf{x}, \mathbf{I})$ , if:

- (a) Locations  $\mathbf{x}$  are centroids of the influence areas; (b) the demand density  $\lambda(x)$  is a constant,  $\lambda_i$ , within each influence area; (c) the inbound transportation cost is a concave function of distance; (d) the outbound transportation cost is a convex and (e) increasing function of distance.

**Proof:** Consider an arbitrarily shaped influence area,  $I_i \in \mathbf{I}$ , with a terminal  $i$  located at its centroid  $x_i$ ; see Figure 7. Let  $Z_{D,i}(\mathbf{x}, \mathbf{I})$  and  $Z_{C,i}(A)$  represent the parts of (1) and (2) corresponding to influence area  $i$ , and denote  $s = s(x, x_i)$  for simplicity.

Since the demand density is constant, substitution of (12) into (1) yields:

$$Z_{D,i}(\mathbf{x}, \mathbf{I}) = \int_{I_i} z^i(R(x_i), \lambda_i | I_i |) \lambda_i dx + \int_{I_i} z^o(s, \lambda_i) \lambda_i dx, \quad (14)$$

Likewise, substitution of (13) into (2) yields:

$$Z_{C,i}(A) = \int_{I_i} z^i(R(x), \lambda_i A(x)) \lambda_i dx + \int_{I_i} z^o\left(\frac{2}{3\sqrt{\pi}} \sqrt{A(x)}, \lambda_i\right) \lambda_i dx, \quad (15)$$

If we can prove that

$$Z_{D,i}(\mathbf{x}, \mathbf{I}) \geq Z_{C,i}(A_s), \quad (16)$$

where  $A_s(x)$  is constrained to be a step function; i.e.,  $A_s(x) = |I_i|$ , if  $x \in I_i$ , then (16) would establish that  $Z_D(\mathbf{x}, \mathbf{I}) \geq Z_C(A_s)$ . This would prove the theorem since  $Z_C^*(A^*)$  is the optimum of  $Z_C(A)$  without any constraint; therefore  $Z_C^*(A^*) \leq Z_C(A_s) \leq Z_D(\mathbf{x}, \mathbf{I})$ .

Note that  $Z_{C,i}(A_s)$  can be expressed as:

$$Z_{C,i}(A_s) = \int_{I_i} z^i(R(x), \lambda_i | I_i) \lambda_i dx + \int_{I_i} z^o\left(\frac{2}{3\sqrt{\pi}} \sqrt{|I_i|}, \lambda_i\right) \lambda_i dx. \quad (17)$$

To prove (16) we first show that the first term of  $Z_{D,i}(\mathbf{x}, \mathbf{I})$  bounds from above the first term of  $Z_{C,i}(A_s)$ . This is clear if we compare the first terms of (14) and (17), because  $R(x_i)$  is the average of  $R(x)$  by assumption (a), and Jensen's inequality suggests (assumption (c)) that:

$$\int_{I_i} z^i(R(x_i), \lambda_i | I_i) \lambda_i dx \geq \int_{I_i} z^i(R(x), \lambda_i | I_i) \lambda_i dx. \quad (18)$$

Thus, to prove (16) we only have to show that the second term of (14) bounds from above the second term of (17); i.e., that

$$\int_{I_i} z^o(s, \lambda_i) \lambda_i dx \geq \int_{I_i} z^o\left(\frac{2}{3\sqrt{\pi}} \sqrt{|I_i|}, \lambda_i\right) \lambda_i dx = \lambda_i |I_i| \cdot z^o\left(\frac{2}{3\sqrt{\pi}} \sqrt{|I_i|}, \lambda_i\right). \quad (19)$$

Note as a preliminary step that:

$$\int_{I_i} z^o(s, \lambda_i) \lambda_i dx \geq \int_{I_i} z^o(\bar{s}, \lambda_i) \lambda_i dx, \quad (20)$$

where  $\bar{s}$  is the average outbound delivery distance in  $I_i$ . This is true, again, by virtue of assumption (d) and Jensen's inequality.

We now define a point-to-point mapping  $\{M: y=M(x), x \in I_i, y \in I_i'\}$ , that transforms  $I_i$  into a round area  $I_i'$  with the same centroid and the same area, and such that  $s'(y, x_i) \leq s(x, x_i)$  for  $\forall y=M(x)$ ; see Figure 8. [This last condition is trivially satisfied by specifying that all points in  $I_i \cap I_i'$  should be fixed points; i.e.,  $y = x$ .] We consider now the cost of serving the transformed region if the demand density in it is still  $\lambda_i$ . Clearly, the inbound costs stay the same. Obviously,

$$\bar{s}' \leq \bar{s}, \quad (21)$$

where  $\bar{s}' = \frac{2}{3\sqrt{\pi}} \sqrt{|I_i'|} = \frac{2}{3\sqrt{\pi}} \sqrt{|I_i|}$  is the average outbound delivery distance in  $I_i'$ . We

can now write:

$$\int_{I_i} z^o(s, \lambda_i) \lambda_i dx \geq \int_{I_i} z^o(\bar{s}, \lambda_i) \lambda_i dx \geq \int_{I_i'} z^o(\bar{s}', \lambda_i) \lambda_i dx = \lambda_i |I_i| \cdot z^o\left(\frac{2}{3\sqrt{\pi}} \sqrt{|I_i|}, \lambda_i\right), \quad (22)$$

where the first inequality is (20), the second inequality follows from (21) and assumption (e), and the final equality follows from the fact that  $|I_i| = |I_i'|$ . This completes the proof. ■

This theorem is valid for any  $N$  and any partition of  $S$ . Of course, it is based on idealized conditions that are quite unrealistic if strictly enforced--since the cost

conditions may not apply in many cases, and demand density will rarely be constant in every influence area. However, we are often faced with problems for which these conditions are approximately true, such as our examples. In these cases the conditions of the theorem should hold, at least approximately. This is confirmed by the numerical results of Section 3, which were not coincidental.

## **5. CONCLUSION**

This paper proposed an automated algorithm to obtain discrete designs out of the continuum approximation recipes for location problems. It can be easily extended to other logistics problems. Numerical results show that the algorithm systematically finds feasible discrete terminal designs with costs very close to those predicted.

The algorithm was illustrated with Euclidean metrics and circular disks. However, it can easily be extended to other metrics and/or applications that require elongated influence areas. Recall too that our algorithm looks for centrally located terminals. There are systems, however, for which terminals should not be at the center of their influence areas; e.g. newspaper distribution systems, where it is advantageous to locate drop-off spots on the edge of their delivery districts (see Daganzo, 1984). In these cases the algorithm should be modified too.

The study also validates the CA cost predictions, by comparing them with the costs for actual designs. The CA prediction is shown to be an approximate lower bound of the true optimum under certain conditions, and to be quite close to the costs of feasible designs. In these cases the CA method produces solutions with a small optimality gap.

**ACKNOWLEDGEMENTS**

This research is supported in part by a research grant from the University of California Transportation Center (UCTC).

**REFERENCES**

1. Okabe, A., Boots, B. and Sugihara, K. (1992). *Spatial Tessellations: Concepts and Applications of Voronoi Diagrams*. Wiley, Chichester, UK.
2. Du, Q., Faber, V. and Gunzburger, M. (1999) “Centroidal Voronoi tessellations: applications and algorithms”, *SIAM Review*, 41(4): 637-676.
3. Daskin, M.S. (1995) *Network and Discrete Location: Models, Algorithms and Applications*, Wiley, New York, USA.
4. Drezner, Z. and Hamacher, H.W. (2002) *Facility Location: Applications and Theory*. Springer, Berlin, Germany.
5. Newell, G.F. (1971) “Dispatching policies for a transportation route,” *Transportation Science* **5**, 91-105.
6. Newell, G.F. (1973) “Scheduling, location, transportation and continuum mechanics: some simple approximations to optimization problems”, *SIAM J. Appl. Math.* 25(3): 346-360.
7. Daganzo, C.F. and Newell, G.F. (1986). “Configuration of physical distribution networks”, *Networks*, 16: 113-132.
8. Daganzo, C.F. (1999). *Logistics System Analysis, 3<sup>rd</sup> Edition*. Springer, Berlin, Germany.
9. Hori, H. and Nagata, M. (1985) “Examples of optimization methods for environment monitoring systems”, *Report B-266-R-53-2, Environmental Sciences*, Ministry of Education, Japan, 18-29 (in Japanese).

10. Daganzo, C.F. (1984). "The distance traveled to visit N points with a maximum of C stops per vehicle: an analytic model and an application", *Transportation Science*, 18(4): 331-350.

**LIST OF FIGURES**

FIGURE 1. Disks and terminals: (a) an infeasible overlapping pattern; (b) a feasible non-overlapping pattern.

FIGURE 2. Two possible layouts of 7 disks in a hexagon: (a) homogeneous pattern; (b) inhomogeneous pattern.

FIGURE 3. Possible definitions of forces: (a) repulsive force for terminal pair  $(i, j)$ ; (b) boundary force for terminal  $i$ .

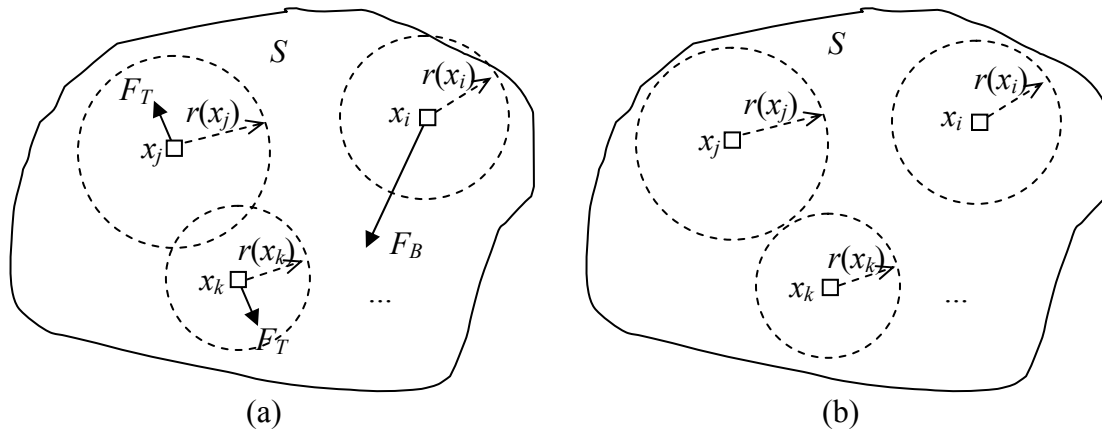
FIGURE 4. Verification of convergence: (a) area  $S$ ; (b) initial locations; (c) locations after 200 iterations; (d) equilibrium locations after 440 iterations.

FIGURE 5. Terminal designs for homogeneous customer demand: (a)  $L=5$ ; (b)  $L=7$ ; (c)  $L=10$ ; (d)  $L=25$ .

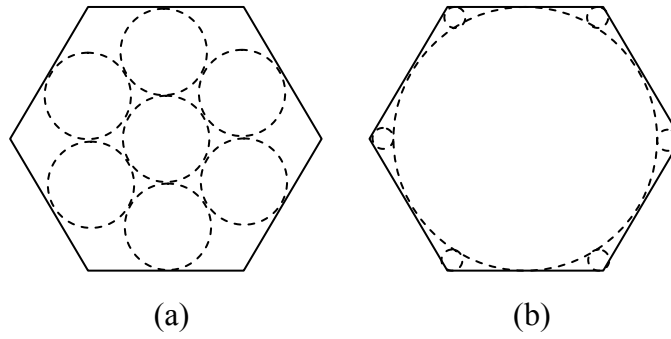
FIGURE 6. Terminal designs for inhomogeneous customer demand: (a)  $L=5$ ; (b)  $L=7$ ; (c)  $L=10$ ; (d)  $L=25$ .

FIGURE 7. Logistic operations in  $I_i$ .

FIGURE 8. Mapping points from  $I_i$  into a round area  $I_i'$ .



**FIGURE 1** Disks and terminals: (a) an infeasible overlapping pattern; (b) a feasible non-overlapping pattern.



**FIGURE 2** Two possible layouts of 7 disks in a hexagon: (a) homogeneous pattern; (b) inhomogeneous pattern.

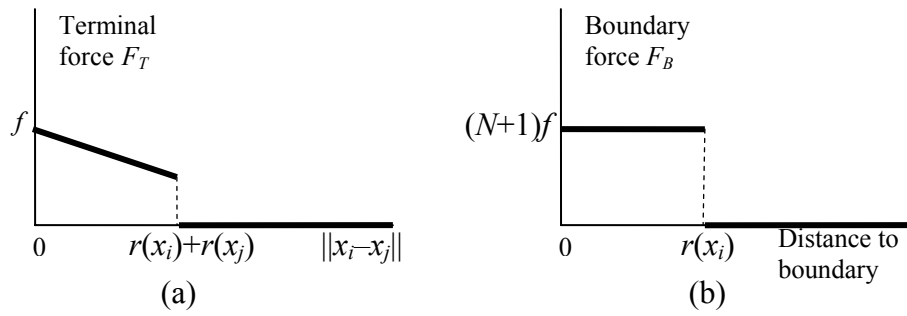


**FIGURE 3** Possible definitions of forces: (a) repulsive force for terminal pair  $(i, j)$ ; (b) boundary force for terminal  $i$ .

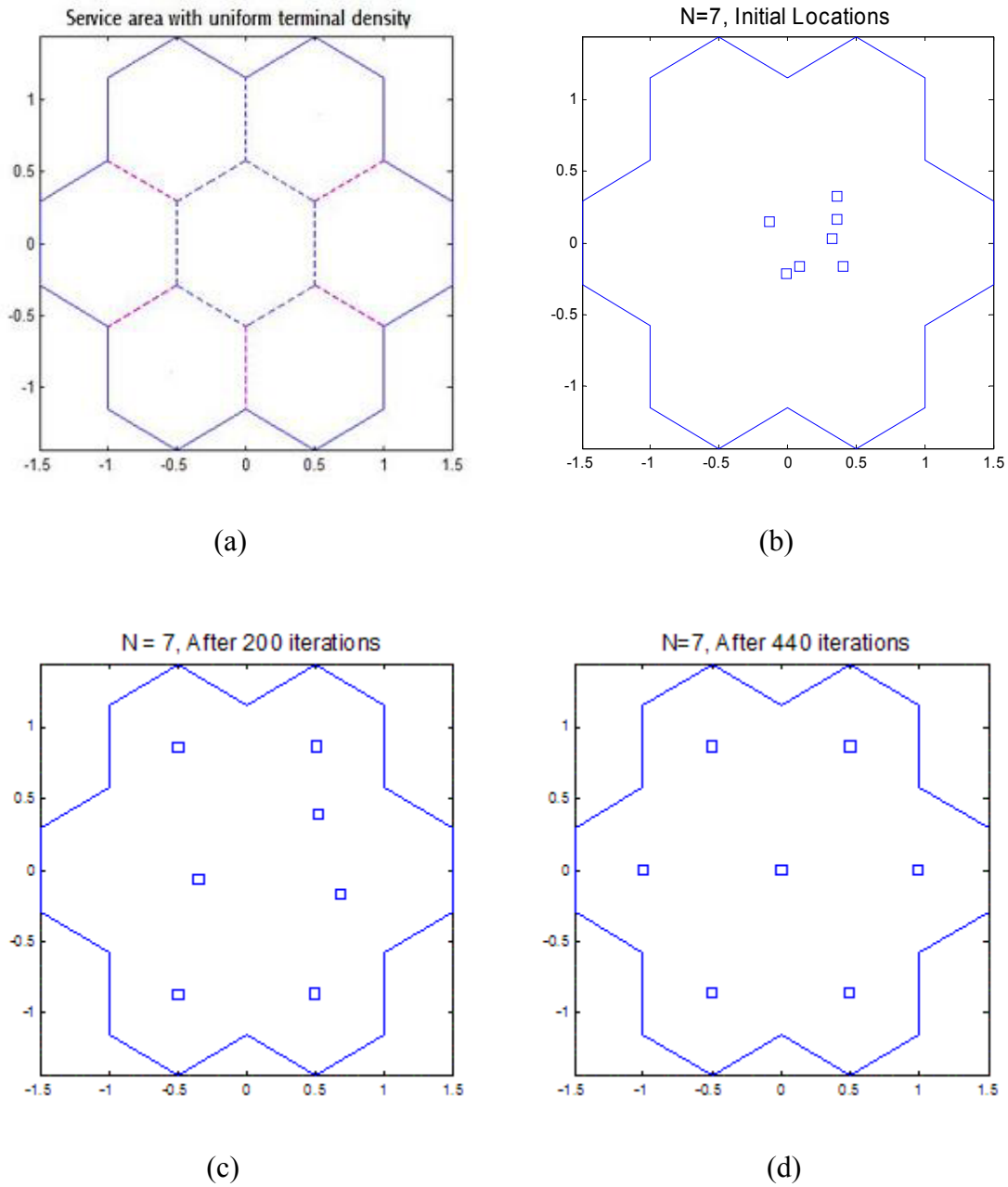
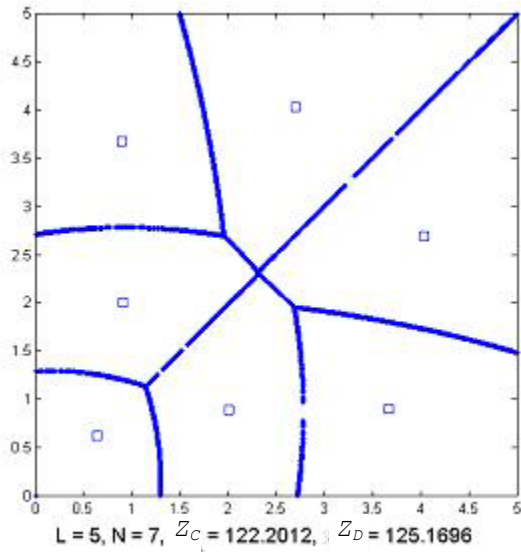
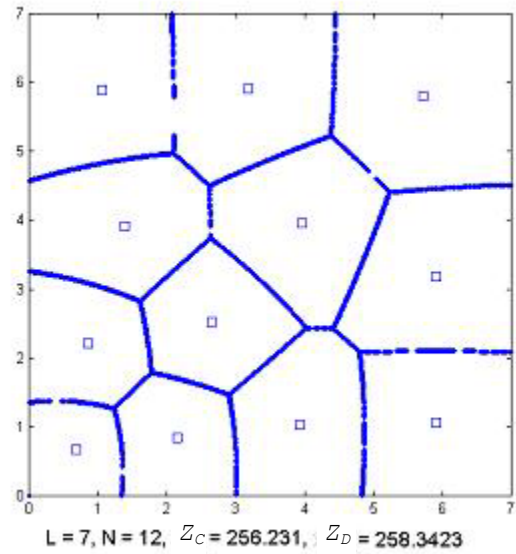


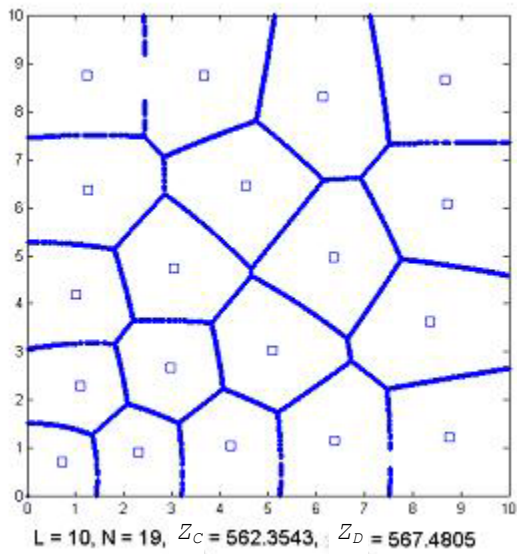
**FIGURE 4** Verification of convergence: (a) area  $S$ ; (b) initial locations; (c) locations after 200 iterations; (d) equilibrium locations after 440 iterations.



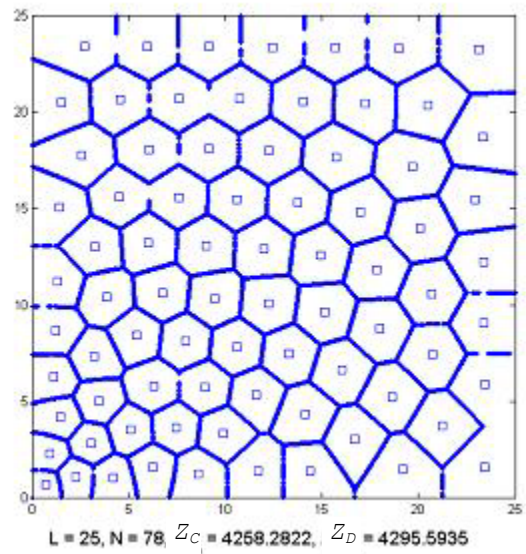
(a)



(b)

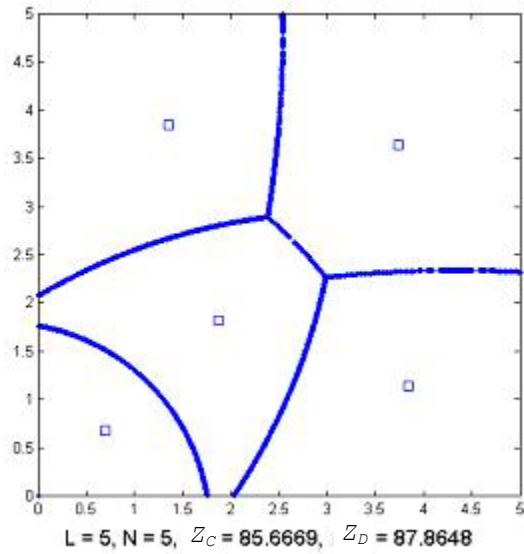


(c)

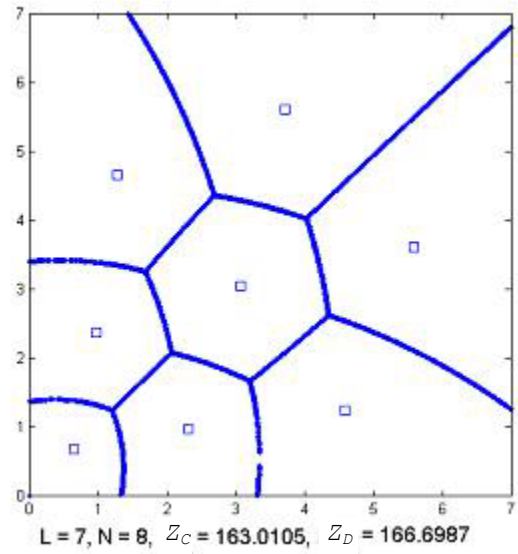


(d)

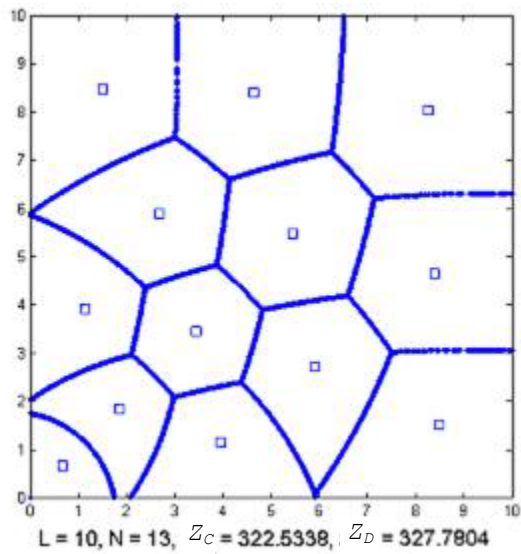
**FIGURE 5 Terminal designs for homogeneous customer demand: (a)  $L=5$ ; (b)  $L=7$ ; (c)  $L=10$ ; (d)  $L=25$ .**



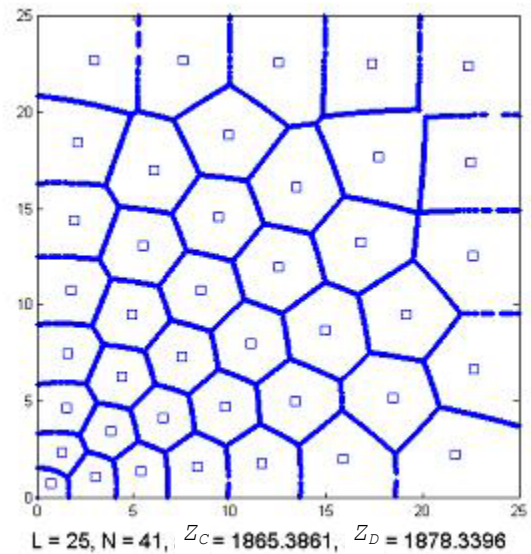
(a)



(b)



(c)



(d)

**FIGURE 6 Terminal designs for inhomogeneous customer demand: (a)  $L=5$ ; (b)  $L=7$ ; (c)  $L=10$ ; (d)  $L=25$ .**

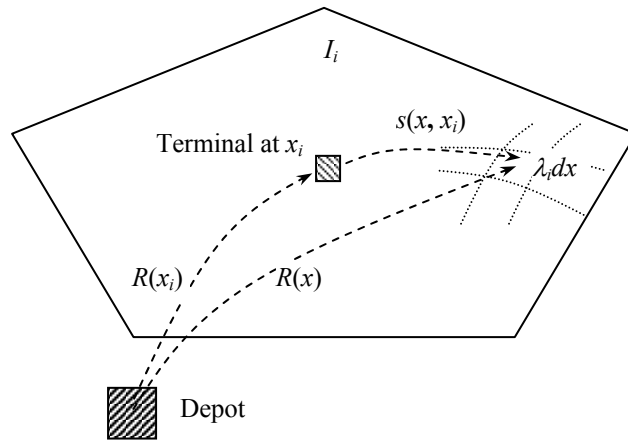


**FIGURE 7** Logistic operations in  $I_i$ .

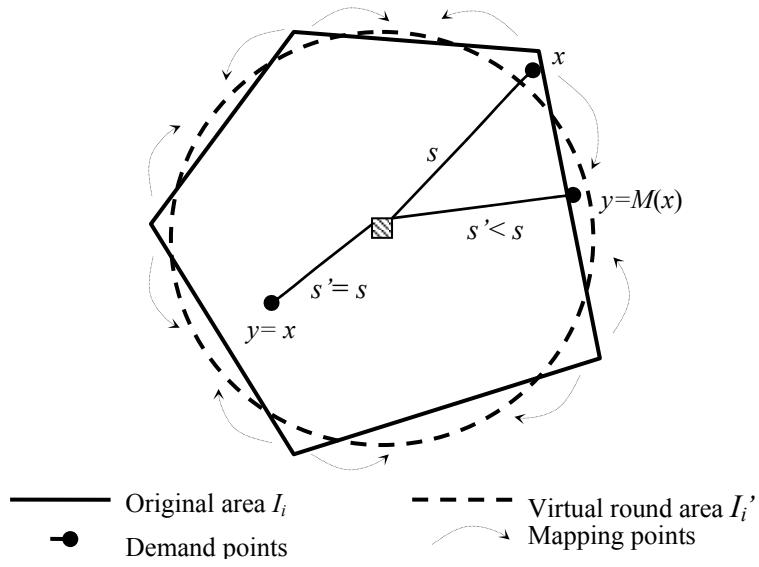


**FIGURE 8** Mapping points from  $I_i$  into a round area  $I_i'$ .